

Exploration of links between Alzheimer's Disease and Depression through 3-dimensional reconstructions of neuropil in hippocampus of aged-impaired and young rats

Maria Dolak¹

¹University of Texas at Austin, Texas, 78712

Abstract (Word count: 120)

The analysis of the structure of neuronal components is often a first step to understand their function. Serial section Transmission Electron Microscopy (ssTEM) provides high resolution of the tissue, thereby allowing for close investigation of synaptic organization including subcellular components. ssTEM combined with a Reconstruct software was used in this study to trace and reconstruct a dendritic shaft with its three spines, synapses, presynaptic axons with vesicles, subcellular components and astroglia. 3-dimensional electron microscopy reconstructions (3DEM) were made in order to show the sizes and locations of these structures, relative to each other. Increasing knowledge about physical organization of neuronal structures can help us understand mechanisms of synaptic transmission. Moreover, morphological changes can be used to predict functional deficits in diseases.

Introduction (Word count: 590)

Cognitive decline is a natural consequence of aging and typically involves a reduction in neuronal arborization and connectivity (Petralia et al., 2014). An increase in synaptic size and number of mature, perforated synapses in aged animals was suggested to be a homeostatic response to reduced synaptic density (Cali et al., 2018). However, an excessive neurodegeneration of immature, nonperforated synapses leads to a decrease in plasticity, which is a characteristic of Alzheimer's Disease (AD) (Neuman et al., 2014). AD is a neurodegenerative disorder impairing spatial recognition and memory. In 2015 AD affected ~ 50 millions of the world's population and is estimated to affect ~80 millions by 2030 (WHO), not including the impact it has on the care-providers.

Depression was reported to be the most frequent psychiatric complication of AD, affecting even up to 50% of patients (Lyketsos and Olin, 2002). The actual prevalence data is most likely lower, with the data ranging from 9.8% to 43.7%, and the discrepancies are due to differences between clinical diagnostic criteria used (Vilalta-Franch et al., 2006). The symptoms' overlap makes it hard to definitively indicate depression in AD patients (Brockman et al., 2011), which requires further investigation of the source of both pathologies. Additionally, people with history of depression, particularly its early onset, show higher odds of developing AD (Geerlings et al., 2008). The association between these two diseases is not yet known. Depression could be an early symptom of AD or an emotional response to decreasing cognitive capacities. However, the importance of *early* depression onset as a predictor of dementia manifestation years later, is in favor of a hypothesis that depression exploits brain reserves early-on, which significantly accelerates cognitive dysfunctions accompanying aging (Jorm, 2001).

Intriguingly, both diseases are associated with mitochondrial dysfunctions. Mitochondria are responsible for ATP production, calcium homeostasis and apoptotic signaling (Moreira et al., 2010). They are generators of reactive oxygen species (ROS) but also a target of it. Increased oxidative stress can lead to dysfunction of mitochondria. This leads to accumulation of ROS, which in turn, further increases mitochondrial oxidative damage. The cycle continues until the cell does not meet energetic requirements and dies (Baloyannis, 2006). Oxidative stress plays an important role in AD and occurs before AB plaque formation (Moreira et al., 2010). Ultrastructural studies have found that neurons in AD animal models show less numerous and significantly elongated mitochondria (Baloyannis, 2006). It was suggested that

this could serve as a protective adaptation to chronic oxidative stress through a decrease of mitochondrial respiration rate (Wang et al., 2008).

Similar mitochondria/ROS cycle and a decrease in ATP production was implicated in molecular mechanisms of depression (Caruso et al., 2019), (Manji et al., 2012). Moreover, it results in mtDNA polymorphism and an increase in mutation rate, both of which were linked with depressive disorders in genetic studies (Manji et al., 2012) Finally, ultrastructural images of cortex, hippocampus and hypothalamus in animal models of chronic mild stress show damaged, swollen mitochondria with broken cristae or incomplete membranes (Gong et al., 2011).

There are apparent similarities in the mitochondrial dysfunction in both AD and depression. One possible explanation is that oxidative stress induced during early-onset depression burdens neuronal regenerative mechanisms, which results in pathologically accelerated effects of aging leading to dementia. To explore this idea, it is important to understand the differences in mitochondrial structure and its effects on synapses between aged-impaired, young depressed and young adult (control) rats. We present three dimensional reconstructions of dendritic shafts with associated boutons and subcellular structures comparing young adult and aged-impaired rat hippocampus towards this goal.

Methods (Word count: 298)

Behavioral Tests

Over 25-months-old (aged) Long Evans rats were examined for cognitive deficits using Morris Water Maze (MWM). Following habituation with experimenters and water tub, each rat had 22 trials over 3 days to learn where an invisible platform is located. There were visual cues placed in each quarter of the tub and the trials' starting point was changing. Day 4 was the probe day where platform was removed. The total distance and amount of time spent in the correct quarter was counted along the number of the platform's area crossings. Cued learning on the day 5 involved cues placed directly on the platform and a changing platform's position, in order to ensure the test measures memory deficits, not visual acuity or locomotor abilities. The MWM data were used to establish discrimination index indicating which of the aged rats had impaired memory. Brains of these and young animals were further examined by students blinded to an animal group.

Subcellular components

The brain of was rapidly fixed through transcardial perfusion with an aldehyde. The tissue from CA1 hippocampal area was vibra-sliced at ~70 µm, the specimen was treated with osmicate, uranyl acetate and lead citrate consecutively to stain proteins. Then, it was dehydrated with acetone for use in the high vacuum of an electron microscope. Tissue was infiltrated with plastic resins, placed in a mold and hardened in 60°C for 48 hours. Subsequently, an ultramicrotome was used to prepare ~49 nm thick ultra-sections for imaging in the transmission electron microscope (TEM).

Reconstruction

Reconstruct Software was used to make traces of chosen dendrites with spines, associated axonal boutons, PSDs, mitochondria, SER and spine apparatus (SA). Vesicles were stamped for counting and astroglial cells and endosomes were stamped to indicate their location. 3D models were created out of the traces.

Results (Word count: 300)

The results presented refer to traces of only one dendrite coming from an aged rat with impaired memory. For a brief analysis of compiled class data from each student see supplementary materials (S1).

Synapse size

One dendritic shaft with six spines was traced in order to learn about the location and size of the synapses. 3D reconstructions and 3 representative EM images show 3 large, concave, perforated synapses and 3 smaller, macular ones (Figure 1A-D, Figure 3A). The distribution of the PSD sizes is in line with the preliminary data (Kirk, 2020).

Vesicles – PSD area relationship

Vesicles were stamped and counted to investigate their relationship with PSD's flat area and a role of mitochondria in it. Among all axonal boutons traced, only one was multi-synaptic (Figure 2A, arrow 2) and both of its synapses accounted for its total PSD area (Figure 2B). There was a clear, positive linear correlation between number of non-docked vesicles and the PSD size. Moreover, increasing number of presynaptic mitochondria was positively correlated with both variables. The positive linear correlation disappears when docked vesicles are considered (Figure 3B). However, in case where a smaller PSD had more docked vesicles than a bigger PSD, it had more mitochondria.

Role of endosomes and astrogelia

Impact of astoglia and endosomes' presence on non-docked vesicles – PSD area relationship was investigated. Only one endosome was identified – smooth vesicle – in spine 3 (Figure 4A,C,E). Considering a lack of data, its impact on vesicles-PSD relationship cannot be established. Interestingly, it was the only spine not surrounded by an astroglial cell.

Bigger synapses were surrounded by more than one astroglial cell (Table 1, spine 2 and 4) and an axo-spinal interface was the predominant astoglia type. The two-tone data point indicate a PSD was surrounded by two different astroglial types (Figure 4D).

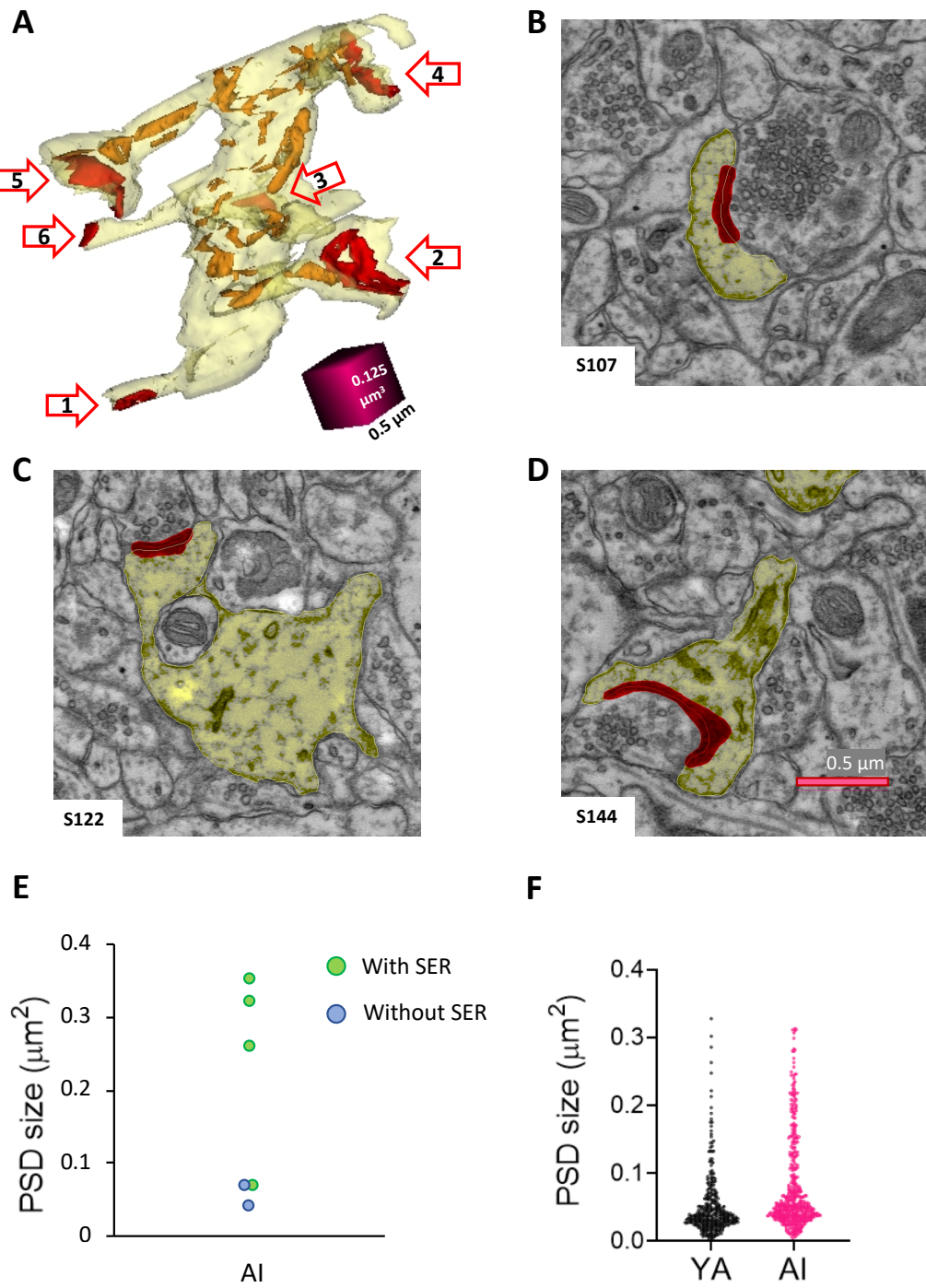


Figure 1. Post Synaptic Density (PSD). (A) 3D reconstruction of a dendritic shaft with its six dendritic spines (yellow) and SER (orange). PSD of each spine shown in red and labeled 1-6 (as indicated by red arrows). 3rd spine is hidden behind the dendritic shaft. (B-D) EM images from sections 107, 122 and 144 showing spines 2,3 and 5 respectively (yellow) and their PSDs (red). (E) Graph presenting an effect of SER presence in a dendritic spine on PSD size in aging rats with impaired memory. (F) Reference graph with distribution of PSD sizes in young adult and aging impaired rats (Dr. Kirk's preliminary data). 0.125 μm^3 (edge = 0.5 μm) cube for scale in the panel A and the 0.5 μm scale-bar on the panel D for all EM pictures.

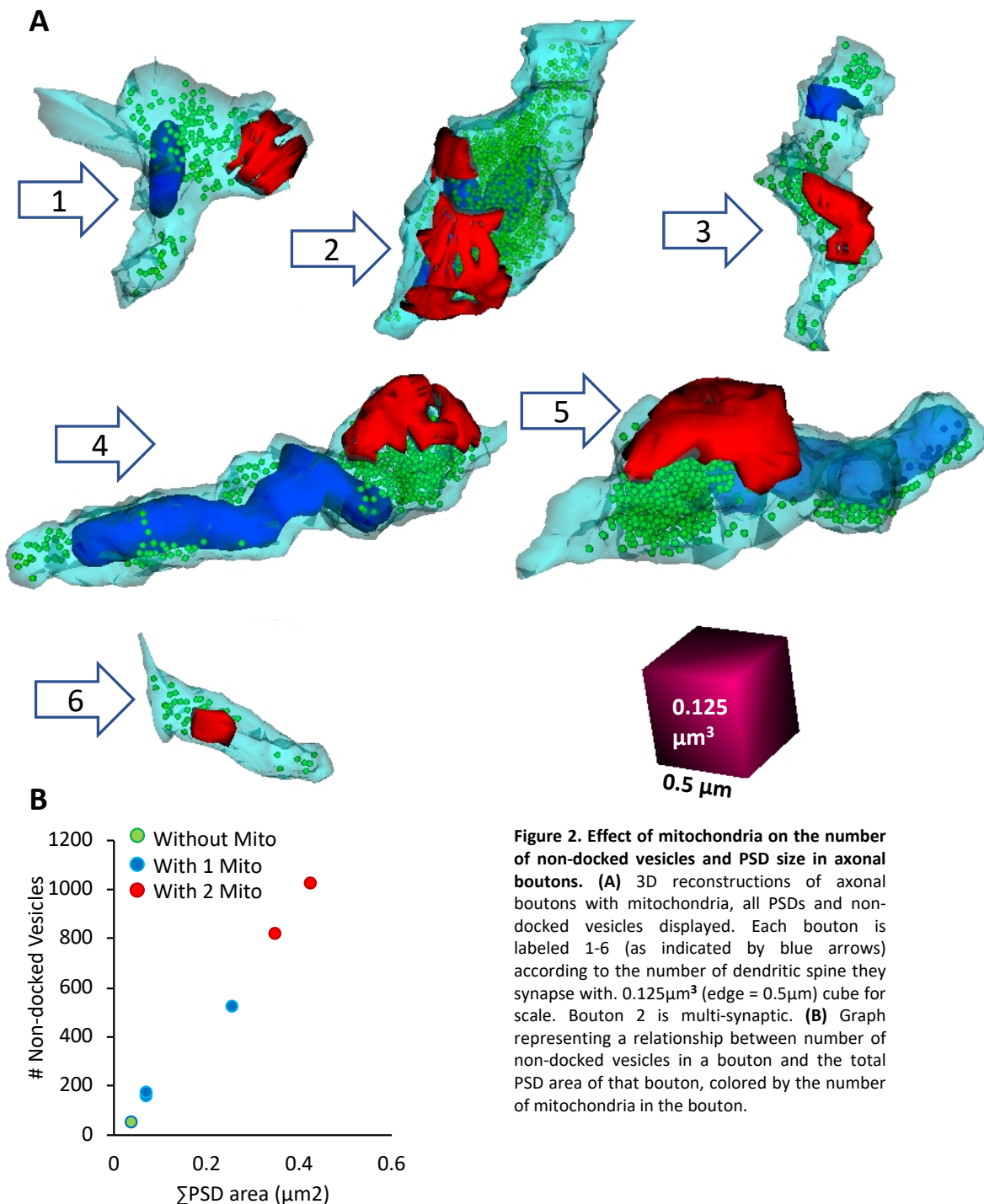


Figure 2. Effect of mitochondria on the number of non-docked vesicles and PSD size in axonal boutons. (A) 3D reconstructions of axonal boutons with mitochondria, all PSDs and non-docked vesicles displayed. Each bouton is labeled 1-6 (as indicated by blue arrows) according to the number of dendritic spine they synapse with. $0.125\mu\text{m}^3$ (edge = $0.5\mu\text{m}$) cube for scale. Bouton 2 is multi-synaptic. (B) Graph representing a relationship between number of non-docked vesicles in a bouton and the total PSD area of that bouton, colored by the number of mitochondria in the bouton.

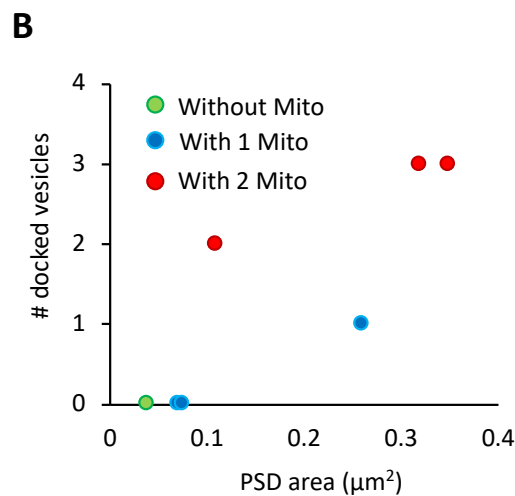
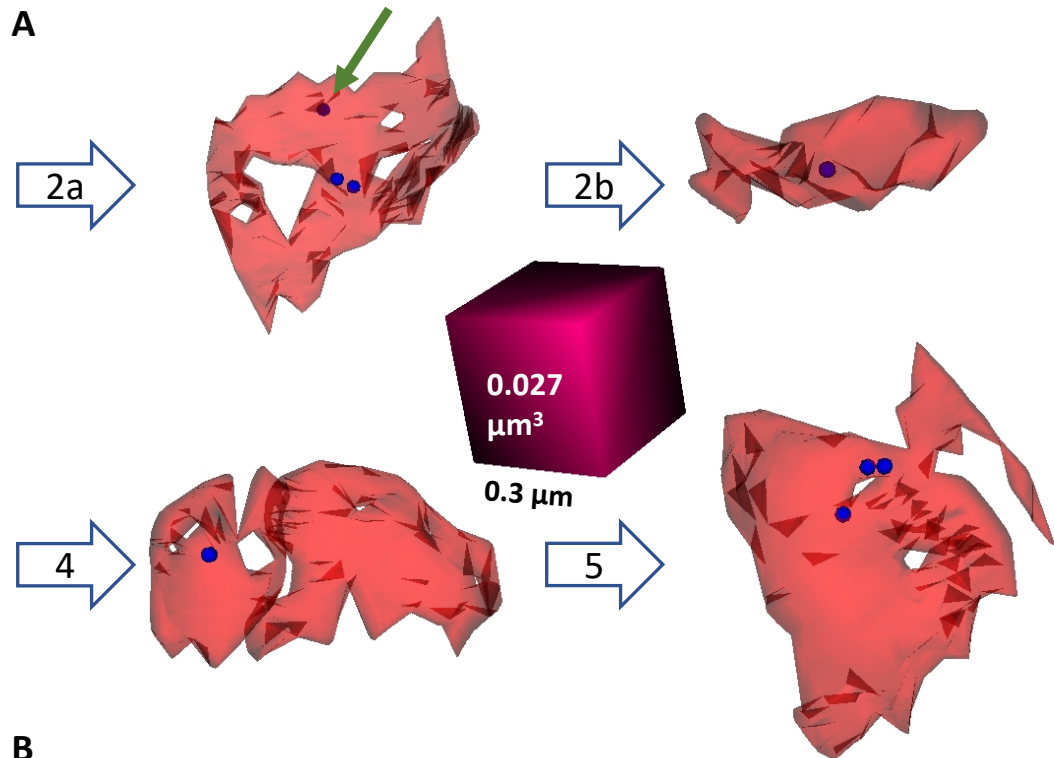


Figure 3. Effect of mitochondria on the number of docked vesicles and PSD size. (A) 3D reconstructions of PSDs from boutons 2,4 and 5 indicated by blue arrows. Both PSDs on a multi-synaptic axonal bouton 2 had docked vesicles (2a and 2b). Green arrow indicates a less visible docked vesicle on the PSD 2a. $0.027\mu\text{m}^3$ (edge = $0.3\mu\text{m}$) cube for scale. (B) Graph representing a relationship between number of docked vesicles and the flat area of a corresponding PSD, colored by the number of mitochondria in the bouton. There were no docked vesicles in three out of the seven traced synapses.

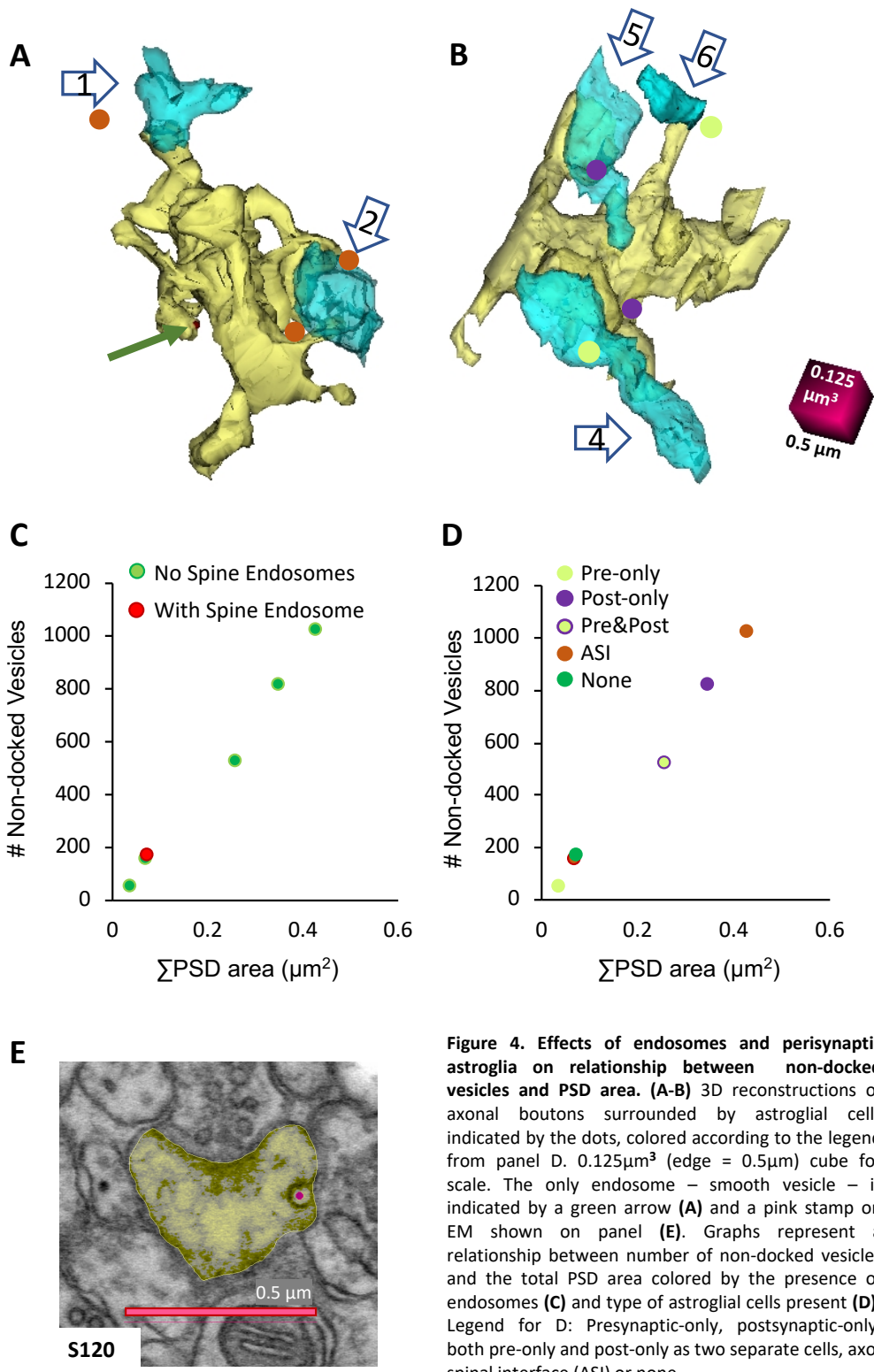


Figure 4. Effects of endosomes and perisynaptic astroglia on relationship between non-docked vesicles and PSD area. **(A-B)** 3D reconstructions of axonal boutons surrounded by astroglial cells indicated by the dots, colored according to the legend from panel D. $0.125\mu\text{m}^3$ (edge = $0.5\mu\text{m}$) cube for scale. The only endosome – smooth vesicle – is indicated by a green arrow **(A)** and a pink stamp on EM shown on panel **(E)**. Graphs represent a relationship between number of non-docked vesicles and the total PSD area colored by the presence of endosomes **(C)** and type of astroglial cells present **(D)**. Legend for D: Presynaptic-only, postsynaptic-only, both pre-only and post-only as two separate cells, axo-spinal interface (ASI) or none.

Table 1. Quantitative summary of all synapses traced.

Object Name	Syn 1	Syn 2	Syn 3	Syn 4	Syn 5	Syn 6	Syn 7 (MSB)
SynArea (Cfa)	0.0718	0.3155	0.0747	0.2598	0.3474	0.0374	0.1129
#Docked Vesicles	0	3	0	1	3	0	2
#Non- Docked Vesicles	154	1021	167	520	814	46	_____
SER tubule in spine (yes/no)	No	Yes	Yes (s122)	Yes	Yes	No	_____
Spine apparatus in spine (Yes/no)	No	Yes	No	Yes	Yes	No	_____
Endosome type in spine (or none)	None	None	Smooth vesicle	None	None	None	_____
Perisynaptic Astroglia status	Pre-only, ASI	2 ASI	None	Post-only, Pre-only	Post-only	Pre-only	_____
Pre-synaptic Mitochondria	1	2	1	1	2	None	2
Perforation	No	Yes	No	Yes	Yes	No	No

Discussion (Word count: 241)

The size of all synapses traced ranges from $\sim 0.04\mu\text{m}^2$ to $0.35\mu\text{m}^2$, with a mean of $0.125\mu\text{m}^2$, which is in line with the preliminary data collected by Dr.Kirk (Kirk, 2020) as well as the dataset collected from all students (S1). The 3D reconstructions revealed elongated presynaptic mitochondria, lack of docked vesicles associated with PSDs when mitochondria were absent and positive correlation between number of mitochondria, number of non-docked vesicles and PSD's flat area. There is no significant impact of endosomes or type of perisynaptic astroglia on vesicles/PSD-area relationship. It might suggest that the role of mitochondria is a more prominent factor in determining the dendritic and synaptic morphology and hence cognitive deficits in aged rats. Nevertheless, a bigger data sample is needed to reach any conclusions.

The methodology of 3DEM presented in this article can serve as a prototype for a bigger data sample. When compared with brains of young rats, it can be a powerful tool in establishing a role of mitochondria

in AD animal models. Besides the presented quantification, it allows for qualitative analysis of mitochondrial structure (not analyzed here).

Despite pharmacological, genetic and molecular evidence for a role of mitochondria in depressive disorders, the ultrastructural changes in these pathologies are still to be explored. In the light of studies showing higher odds of AD onset in people with history of depression, 3DEM mitochondrial analysis might be a starting point for discovery of underlying mechanisms interconnecting these two diseases, thereby improving diagnosis and targeting treatments.

I thank Christian Wintz for reading the paper and providing insightful editorial comments.

References

- Baloyannis S (2006) Mitochondrial alterations in Alzheimer's disease. *Journal of Alzheimer's Disease* 9:119-126.
- Brockman S, Jayawardena B, Starkstein S (2011) The diagnosis of depression in Alzheimer's disease: review of the current literature. *Neuropsychiatry* 1:377-384.
- Calì C, Wawrzyniak M, Becker C, Maco B, Cantoni M, Jorstad A, Nigro B, Grillo F, De Paola V, Fua P, Knott G (2018) The effects of aging on neuropil structure in mouse somatosensory cortex—A 3D electron microscopy analysis of layer 1. *PLOS ONE* 13:e0198131.
- Caruso G, Benatti C, Blom J, Caraci F, Tascedda F (2019) The Many Faces of Mitochondrial Dysfunction in Depression: From Pathology to Treatment. *Frontiers in Pharmacology* 10.
- Geerlings M, den Heijer T, Koudstaal P, Hofman A, Breteler M (2008) History of depression, depressive symptoms, and medial temporal lobe atrophy and the risk of Alzheimer disease. *Neurology* 70:1258-1264.
- Gong Y, Chai Y, Ding J, Sun X, Hu G (2011) Chronic mild stress damages mitochondrial ultrastructure and function in mouse brain. *Neuroscience Letters* 488:76-80.
- Jorm A (2001) History of Depression as a Risk Factor for Dementia: An Updated Review. *Australian & New Zealand Journal of Psychiatry* 35:776-781.
- Kirk L (2020) The synaptic architecture of cognitive decline with aging.
- Lyketsos C, Olin J (2002) Depression in Alzheimer's disease: overview and treatment. *Biological Psychiatry* 52:243-252.
- Manji H, Kato T, Di Prospero N, Ness S, Beal M, Krams M, Chen G (2012) Impaired mitochondrial function in psychiatric disorders. *Nature Reviews Neuroscience* 13:293-307.
- Moreira P, Carvalho C, Zhu X, Smith M, Perry G (2010) Mitochondrial dysfunction is a trigger of Alzheimer's disease pathophysiology. *Biochimica et Biophysica Acta (BBA) - Molecular Basis of Disease* 1802:2-10.

Neuman K, Molina-Campos E, Musial T, Price A, Oh K, Wolke M, Buss E, Scheff S, Mufson E, Nicholson D (2014) Evidence for Alzheimer's disease-linked synapse loss and compensation in mouse and human hippocampal CA1 pyramidal neurons. *Brain Structure and Function* 220:3143-3165.

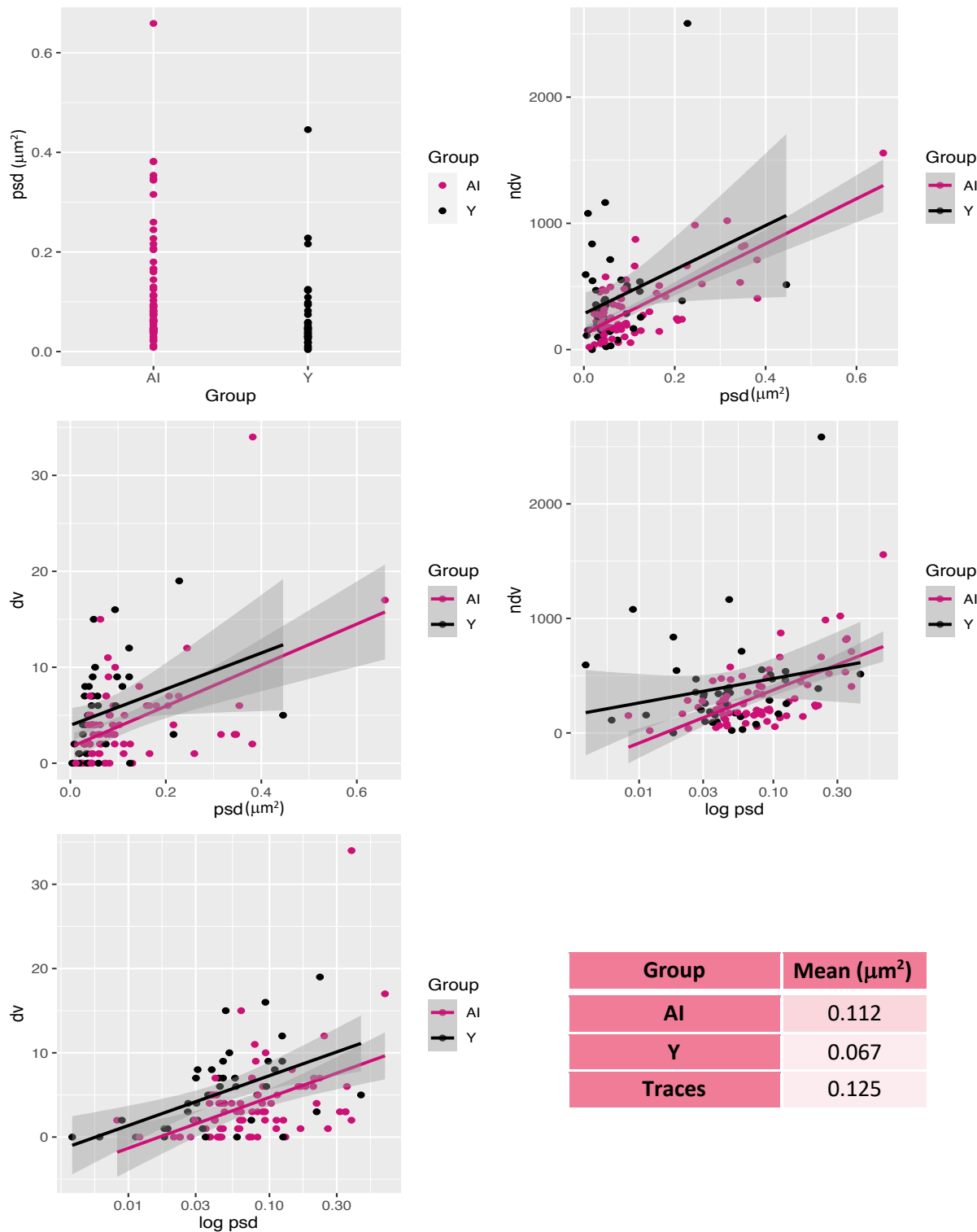
Petralia R, Mattson M, Yao P (2014) Communication breakdown: The impact of ageing on synapse structure. *Ageing Research Reviews* 14:31-42.

Vilalta-Franch J, Garre-Olmo J, López-Pousa S, Turon-Estrada A, Lozano-Gallego M, Hernández-Ferràndiz M, Pericot-Nierga I, Feijóo-Lorza R (2006) Comparison of Different Clinical Diagnostic Criteria for Depression in Alzheimer Disease. *The American Journal of Geriatric Psychiatry* 14:589-597.

Wang X, Su B, Fujioka H, Zhu X (2008) Dynamin-Like Protein 1 Reduction Underlies Mitochondrial Morphology and Distribution Abnormalities in Fibroblasts from Sporadic Alzheimer's Disease Patients. *The American Journal of Pathology* 173:470-482.

WHO. (2017, September 1) Infographic. Dementia, A Public Health Priority. Retrieved 2020, May 8, from https://www.who.int/mental_health/neurology/dementia/infographic_dementia.pdf?ua=1

Supplementary Materials



S1. The collective class data from all students – Aged-Impaired and Young rats. **(A)** PSD size distribution for young (Y, black) and aged-impaired (AI, pink) rats. **(B)** Relationship between number of non-docked vesicles and PSD size with linear regression overlaid, colored by animal group. **(C)** Relationship between number of docked vesicles and PSD size with linear regression overlaid, colored by animal group. **(D)** Relationship between number of non-docked vesicles and natural log of PSD size with linear regression overlaid, colored by animal group. **(E)** Relationship between number of docked vesicles and natural log of PSD size with linear regression overlaid, colored by animal group. **(F)** Table representing mean PSD size for aged-impaired (AI), young (Y) rats and a mean of synapses traced in this paper (Traces).

Software: R; tidyverse library